EFFECTS OF PHASE MIXTURES ON LONG TERM STABILITY OF YTTERBIUM-SILICATE ENVIRONMENTAL BARRIER COATINGS

Eric Stone[a], Dr. Elizabeth Opila[a] (advisor)
[a] University of Virginia, Department of Materials Science & Engineering
Virginia Space Grant Consortium 2021 Student Research Conference

Abstract: Silica-depletion behavior of air plasma spray (APS) fabricated rare-earth (RE) silicate environmental barrier coatings (EBCs) in steam is a valuable research interest for projecting component lifetimes during turbine service. Model phase-mixture samples were created using 5-50 μm ytterbium monosilicate (YbMS) granules dispersed within a ytterbium disilicate (YbDS) matrix for compositions of 10, 20, and 30 volume percent YbMS/YbDS. A modified horizontal tube furnace, termed a "steam-jet", was used for high-temperature (T=1200, 1300, and 1400 °C) high-velocity ($50 \frac{m}{s} < \upsilon < 150 \frac{m}{s}$) water vapor exposures at total pressure of 1 atmosphere. YbDS reacted with high-velocity steam to form a volatile silicon hydroxide gas species and a porous YbMS reaction product that increased in thickness with both increasing time and temperature. For the times, temperatures, and steam velocities analyzed in this study, YbMS granules did not display steam reactivity. At 1200 °C the average SiO_2-depletion reaction depth of all phase-mixtures was similar. For higher test temperatures, average SiO_2-depletion reaction depth was decreased through increasing YbMS second-phase additions, suggesting the relative phase concentration of EBCs can be used to tailor thermochemical stability in combustion environments.

Background and Motivation

Nickel-base superalloy components for aircraft engines currently use cooling air channels to operate at temperatures (T ~ 1300°C) approaching the melting point of nickel (T_m = 1455°C). Hotter combustion chamber temperatures increase fuel efficiency by decreasing specific fuel consumption and promoting more complete fuel combustion. The next-generation of gas-turbine engines will improve overall efficiency by increasing combustion chamber temperatures and shedding engine weight through replacement of heavy metal superalloy components with silicon carbide (SiC) ceramic matrix composites (CMCs).

SiC ceramics and associated silica thermally grown oxide (TGO) are at risk to degrade rapidly when exposed to high-temperature water vapor [1,2], a product of hydrocarbon combustion and the reactive gas species for EBCs in the exhaust stream. To enable use of CMCs in combustion environments, rare-earth (RE) silicate environmental barrier coatings (EBCs) are applied to preclude CMC reaction with the water vapor environment of turbine service.

State-of-the-art EBCs consist of $Yb_2Si_2O_7$, ytterbium disilicate (YbDS), because of its excellent thermal expansion match with SiC and the Si bond coat. A dual-phase mixture of YbDS and Yb_2SiO_5, ytterbium monosilicate (YbMS), as a second-phase inclusion is characteristic of the EBC microstructure produced by the industry standard air plasma spray (APS) process due to SiO(g) volatilization within the plasma plume. YbMS displays highly anisotropic thermal expansion and is unsuitable as a stand-alone EBC candidate. However, YbMS has a lower silica activity than YbDS rendering it more stable in combustion environments [3]. Other works have also observed benefits from additions of YbMS to YbDS. Webster & Opila [4] reported resistance of phase-mixtures to attack by molten calcium-magnesium-alumino-silicate (CMAS), a general compositional category of ash and siliceous debris which can be ingested into engines and infiltrate coatings. Yet, controlled studies of second-phase effects on silica-depletion in steam are lacking in the literature.

This project studies the ytterbium-silicate EBC system comprised of a dual-phase mixture of $Yb_2Si_2O_7$ and Yb_2SiO_5. The effects of phase-

mixture compositions on EBC degradation behavior in steam will be addressed.

The following reaction [5] is isolated through this work:

$$Yb_2Si_2O_7 + 2H_2O\ (g) \rightarrow Yb_2SiO_5 + Si(OH)_4\ (g) \quad (1)$$

Experimental

Two-phase mixture specimens consisting of 10, 20, and 30 volume percent (vol%) ytterbium monosilicate[6] (YbMS) granules, 5-50 μm in diameter, dispersed as a second-phase within a ytterbium disilicate[6] (YbDS) matrix were fabricated at UVA. Powders were weighed and mixed for 5-8 hours using a ball mill prior to preparation for spark plasma sintering (SPS). Fabrication conditions were 65 MPa at 1550 °C for a 15-minute hold time in argon. Post-process annealing was conducted in an ambient-air box furnace at 1500 °C for 24 hours to remove residual carbon from the SPS process and return oxygen stoichiometry. Samples were then wafered and cut into 10mm x 12.5mm x 1mm coupons and polished prior to steam exposures. Examples of the YbMS second-phase distribution within the YbDS matrix is presented in Figure 1 for the two compositional extremes tested, 10 and 30 vol % YbMS in YbDS.

Specimens were exposed to high-velocity (~ 250 m/s) water vapor in a modified horizontal tube furnace, termed a "steam-jet" [6,7,8,9,10], operating with a Pt-Rh capillary and preheater as described by Parker & Opila [10]. De-ionized water was pumped through a 1mm inner-diameter Pt-Rh capillary, passing through a 900 °C preheater. Within the preheater section, water is vaporized and associated volume expansion resulted in high-velocity steam being ejected from the capillary outlet within the tube furnace hot-section. This steam impinges upon the sample face a fixed distance of 1mm from the capillary exit, where the sample is oriented at 45 degrees to the capillary axis. Steam exposures were performed at temperatures of 1200, 1300, and 1400 °C for times of 60, 125, and 250 hours. Specimens were then characterized using X-ray diffraction (XRD) and imaged in plan-view using scanning electron microscopy (SEM) to investigate the surface microstructure of the water vapor impingement site and surrounding area.

Following plan-view imaging, samples were prepared for cross-sectional SEM to visualize the reaction depth. Samples were mounted in epoxy, ground, and polished to obtain cross-sections normal to the primary axis of gaseous flow. Data presented in this work were taken from cross-sections between 3 and 3.5 mm downstream from the center of the impingement site. Analysis of downstream sections increases the sampling length of the area labeled Region (1) in Figure 2.

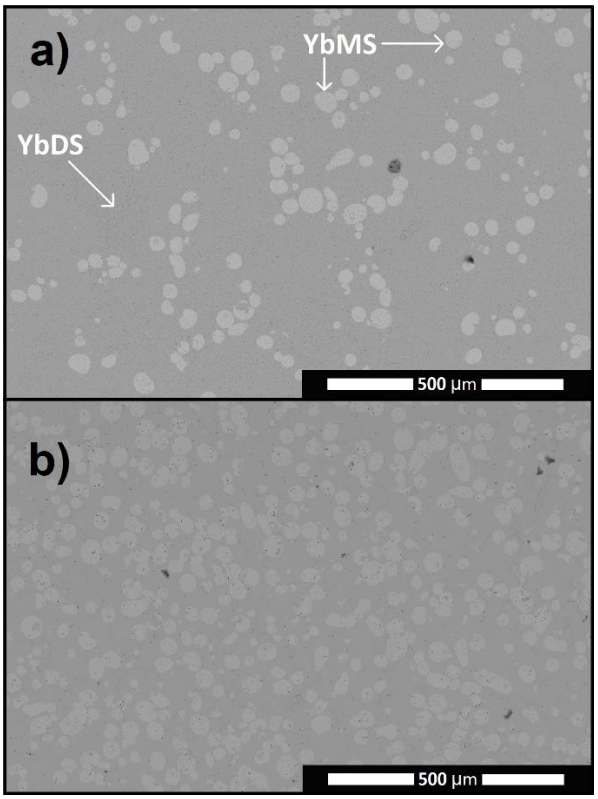

Figure 1: Representative microstructures showing distribution of YbMS second-phase for the two compositional extremes tested: a) 10 vol % YbMS in YbDS and b) 30 vol % YbMS in YbDS.

Extended images were compiled using the ImageJ visual software analysis package from successive individual SEM images. A grid was overlaid upon the image at intervals of

approximately 50 μm. Periodic depth measurements, taken along an area about 1mm in length, were used to obtain an average SiO_2-depletion depth for the reaction layer studied in Region (1). Monitoring the evolution of SiO_2-depletion depth with respect to time gives kinetic rate information about the process. A lower SiO_2-depletion rate indicates decreased reactivity with water vapor and a more stable EBC candidate.

General Results

Visualizing the velocity environment across the sample face helped to better understand the surface environment it experienced. This was accomplished through use of the ANSYS engineering software. Inputs to the program were the steam-jet and sample geometry, water flow rate, and test temperature. The contour of gas-stream velocities for impinging water vapor across the sample face was calculated. An example velocity contour map is shown in Figure 2, calculated at 1400 °C for a cold-water flow rate of 2 mL/min. Since the sample is oriented 45 degrees relative to the capillary outlet, directional flow is reflected by the spreading bell shape of the ANSYS velocity contour map towards "downstream" regions.

The highest steam velocities, shown in red on Figure 2 corresponding to the water vapor impingement site, experienced material loss from apparent mechanical erosion. Surrounding the impingement site is an oval region, overlaid in white on the contour map, which bounds complex behavior found in the inner region experiencing higher velocities above 150 m/s. This region is omitted from current analysis due to increased complexity from such factors as multiple steam reactions, new microstructural changes, and increased mechanical erosion of material.

The region of interest outside this oval, labeled Region 1, isolated Reaction (1). A uniform porous product was formed which increases in depth with increasing temperature and time. By limiting quantitative analysis to Region 1, the effects of YbMS second-phase granules on the kinetic rate of the SiO_2-depletion reaction are illuminated.

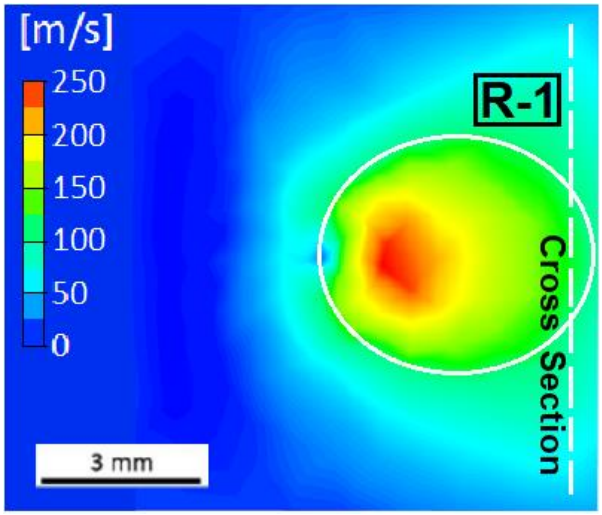

Figure 2: ANSYS velocity contour map for test specimen calculated at 1400 °C, 2.0 ml/min H_2O flow rate, using apparatus and sample geometry. Cross-section position 3-3.5mm downstream from center of impingement site is shown here as sampling a significant length of Region 1 (R-1) behavior experiencing $\upsilon < 150 \frac{m}{s}$.

1200 °C Results

Current results taken from this region target steady-state behavior only complicated by the interaction behavior of interest: second-phase YbMS and Reaction (1) product YbMS. At this temperature, silica-depletion behavior was similar for all compositions tested due to the small length scale, not yet comparable to the granule feature scale. After 250 hours of steam exposure at 1200 °C, the thickness of the YbMS porous layer was approximately 5 μm for expected gas velocities of 50-150 m/s. Figure 3 provides a representative scanning electron micrograph (SEM) image of the silica-depletion depth experienced after 250 hours at 1200 °C. Backscattered electron imaging provided phase contrast that differentiated the underlying YbDS matrix material from lighter YbMS phase. Retention of the original polished surface, seen as the flat tops of dense YbMS,

displayed the lack of reaction from second-phase YbMS granules under Region 1 conditions.

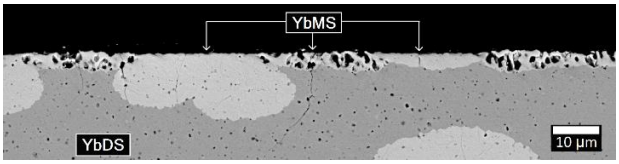

Figure 3: Silica-depletion for a 10 vol% YbMS in YbDS sample exposed at 1200 °C for 250 h in Region 1 of $\upsilon < 150 \frac{m}{s}$.

1300 °C Results

Without local YbMS granules, the expected uniform porous [6] Reaction (1) product was observed, approaching the order of 40 µm in maximum possible depth for test times of 250 h. After high-velocity steam exposures of mixed-phase samples at 1300 °C, the SiO_2-depletion depth was an order of magnitude larger than seen for 1200 °C exposures. The steam reaction depths were comparable to the length scale of YbMS second-phase features after 1300 °C exposures.

Presence of YbMS second-phase granules was determined through identification of fully dense YbMS structures within the porous reaction layer. Many of these second-phase structures were observed to affect continued advancement of the reaction front into the YbDS matrix below.

Figure 4 and Figure 5 display representative instances of the degrees to which YbMS granules can interact with the advancing reaction interface. In some instances, YbMS granules decreased local progression of the reaction interface and therefore decreased the amount of YbDS degradation beneath. The magnitude of this interaction in analyzed samples varied from no effect to pinning the reaction front near the sample surface.

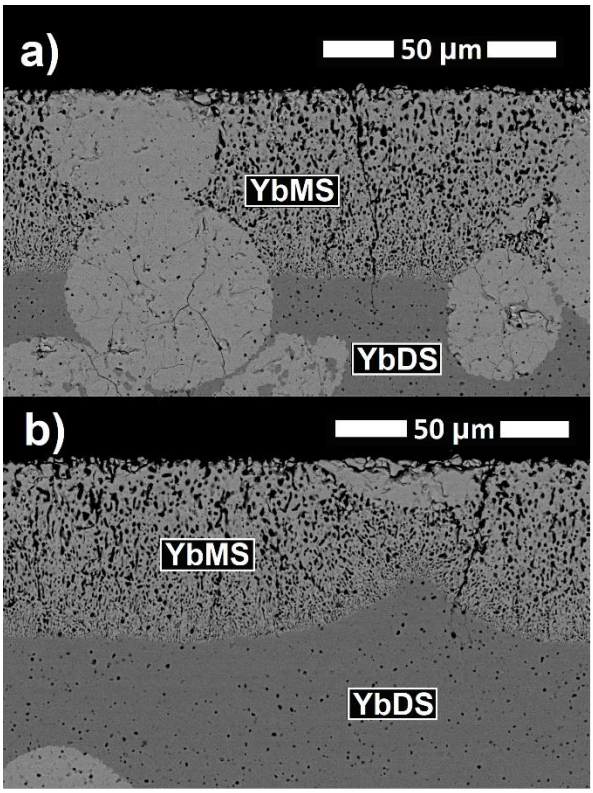

Figure 4: Examples of a) no YbMS second-phase effect on advancing reaction front and b) somewhat reduced silica-depletion depth. Images taken from Region 1 of $\upsilon < 150 \frac{m}{s}$ for a 10 vol % YbMS in YbDS sample exposed at 1300 °C for 250 hours.

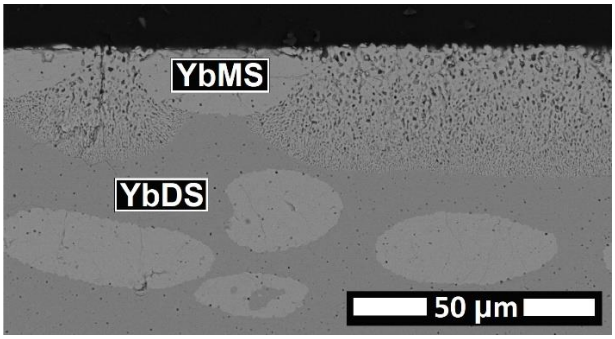

Figure 5: Example of a pronounced reduction in SiO_2-depletion depth resulting from YbMS second-phase interaction with the advancing Reaction (1) interface. Image taken from Region 1 of $\upsilon < 150 \frac{m}{s}$ for a 10 vol % YbMS in YbDS sample exposed at 1300 °C for 125 hours.

Figure 6 displays an extended image of a 10 vol% YbMS in YbDS sample exposed at this temperature for 250 h. Influence of a small local concentration of YbMS second-phase somewhat abated the Reaction (1) interface for this presented portion of Region 1. It was observed that more extensive reduction of reaction depth occurred when YbMS granules were in close proximity to each other. This behavior continues to be evident when referencing higher second-phase concentrations like that shown in Figure 7 for a Region 1 portion of 30 vol % YbMS in YbDS exposed to steam for 250 h. In Figure 7, local clustering of YbMS granules which limited the extent of silica-depletion from the YbDS matrix beneath is highlighted throughout the image center. These two figures presented are only small lengths of the measured portions of Region 1 which are used to build the average reaction depth values.

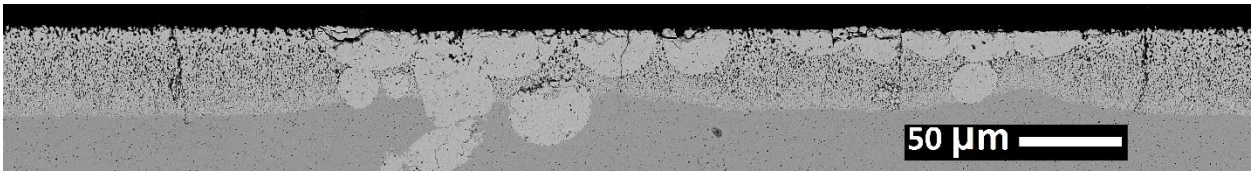

Figure 6: Extended micrograph image of a 3.5mm downstream cross-section from a 10 volume percent YbMS in YbDS sample tested at 1300 °C for 250h in the projected velocity regime of 50-150 m/s. Backscatter electron imaging shows phase contrast between the darker YbDS phase and lighter YbMS.

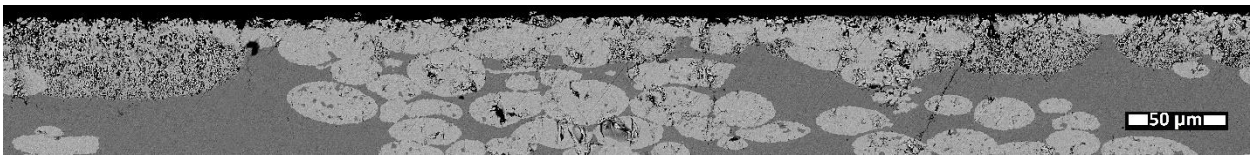

Figure 7: Extended micrograph image of a 3.5mm downstream cross-section from a 30 volume percent YbMS in YbDS sample tested at 1300 °C for 250h in the projected velocity regime of 50-150 m/s. Backscatter electron imaging shows phase contrast between the darker YbDS phase and lighter YbMS. Close-packed YbMS second-phase granules limit underlying YbDS degradation.

A calculated average reaction depth value defines the behavior of the silica-depletion reaction for a phase-mixture composition in steam at an expected gas velocity range of 50 – 150 m/s for this work. Figure 8 compares the time-dependence of 10 vol % YbMS in YbDS and 30 vol % YbMS in YbDS average SiO_2-depletion depth curves at 1300 °C, where the x-axis is presented as the square root of the exposure times. The linear trendlines presented on this graph are indicative of a diffusion-controlled process. This is rationalized through the increasing path length with respect to time of the diffusing $Si(OH)_4$ (g) molecule through the porous network and into the gas boundary layer.

The slope of the trendline for each composition is proportional to the square root of the parabolic rate constant which describes the advancement of the reaction front. A lower slope indicates a slower SiO_2-depletion rate and a more robust EBC material. The averaged SiO_2-depletion behavior of the 30 vol% YbMS in YbDS trendline was consistently lower than the 10 vol% YbMS in YbDS rate for all times tested at 1300 °C, highlighted in Figure 8. Thus, increased concentrations of YbMS second-phase granules in the starting material effectively reduced the average steam reaction rate.

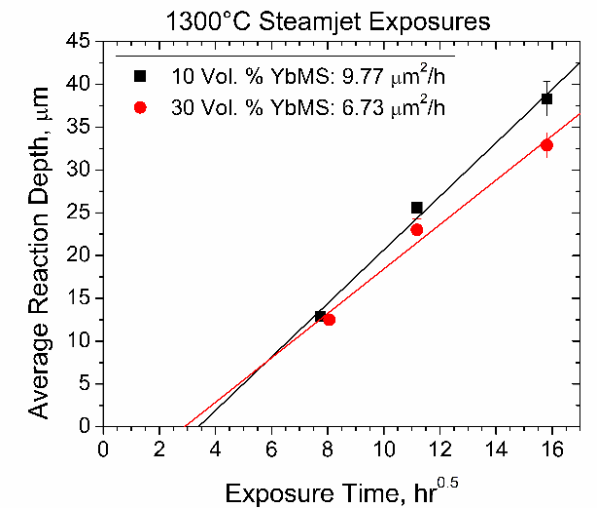

Figure 8: 1300 °C averaged reaction depth versus the square root of exposure time for 10 and 30 vol % YbMS in YbDS compositions to investigate the parabolic growth rate constant as the slope of the presented trendlines squared.

Discussion

High-velocity steam exposures of dual-phase ytterbium silicates at 1200 °C displayed small averaged SiO_2-depletion depths, especially when compared to traditional EBC thicknesses (~200-350 μm) of APS coatings. Although parabolic-limited growth kinetics were supported from 1200 °C analysis, the lower order of SiO_2-depletion depth when compared to higher temperatures is a point of ponderance. Reaction behavior increased by an entire order of magnitude from 1200 to 1300 °C, yet only doubled in maximum possible depth from ~ 40 to ~80 μm during the interval between 1300 and 1400 °C. It has been suggested by Ridley [5] from apparent reaction enthalpy calculations that a different steam reaction mechanism may be at work for 1200 °C exposures.

Alternative applications to turbine engines for temperatures of 1200 °C or lower can benefit from EBCs. Small-scale degradation coupled with a reducing silica-depletion rate over time could indicate possible long component life for alternative applications below 1200 °C such as steam power plant turbines.

The first difference noted upon investigating higher temperatures is the increased reaction depth. Silica-depletion depths for the temperatures and times tested are still less than traditional EBC thicknesses, which supports ytterbium silicate viability as a superior EBC. However, the longest test times in this work (250 h) are still two orders of magnitude less than desired engine life-hours. Therefore, a projected average SiO_2-depletion depth should be calculated for the 10,000 life-hours requirement of turbine service [9]. Using the parabolic reaction rates determined in this work, projection of 30 vol% YbMS in YbDS silica-depletion behavior approximates 260 μm of average material recession in steam after 10,000 hours of continuous service at 1300 °C. This suggests that a YbMS second-phase volume fraction in balance YbDS of 30 vol % is viable to support EBCs for extended operation.

I will now turn to an important point of consideration on stress-states. This work utilizes spark plasma sintering sample fabrication as an in-house means of sample creation. It is important to note that the EBC material coupons produced in this manner have no substrate and therefore generated no related stress state from considerations such as lattice constraint.

A stress-free state is not completely realistic. Although real APS EBC samples with realistic stress states can be exposed, APS EBC fabrication can be difficult and costly to control for particular parameters in small batches. However, future experimentation such as utilizing differing substrates to systematically investigate the effects of varying stress-state on EBC degradation behavior in steam may become a worthwhile pursuit.

In conclusion, it should be noted that this work is preliminary in nature and meant to be used as a bounding case for influence on the experimental system, namely large identifiable second-phase inclusions. Other various bounding

cases of interest might be higher volume fractions of second-phase, varying distributions, in addition to more systematic control over a range of microstructural features.

Conclusion

High-temperature high-velocity steam exposures of YbDS with controlled amounts of YbMS second-phase granule inclusions were analyzed. Fabricated phase-mixture samples were investigated as simplistic models of the complex phase distribution found in APS EBCs used in turbine service. For samples exposed to steam at 1300 °C the averaged parabolic steam reaction rate, represented by the averaged SiO_2-depletion depth with respect to square root of exposure time, was found to decrease with increasing volume % of YbMS second-phase inclusions. The EBC silica-depletion rate in steam can thus be tailored through controlling phase-fraction and distribution to increase coating lifetimes in service.

Acknowledgements

This work was supported by Rolls-Royce corporation and supervised by program manager Dr. Stephanie Gong. Additional support is thanks to the Virginia Space Grant Consortium (VSGC) 2020-2021 graduate research fellowship program. Finally, I would like to acknowledge the facilities and insight from the University of Virginia (UVA) Nanoscale Materials Research Facility (NMCF).

References

1. Opila EJ, Hann RE. Paralinear Oxidation of CVD SiC in Water Vapor. Journal of the American Ceramic Society. 1997;80(1):197–205. https://doi.org/10.1111/j.1151-2916.1997.tb02810.x

2. Opila EJ. Variation of the Oxidation Rate of Silicon Carbide with Water-Vapor Pressure. Journal of the American Ceramic Society. 1999. 82(3):625-636.

3. Gustavo C, Jacobson NS. Mass spectrometric measurements of the silica activity in the Yb2O3– SiO2 system and implications to assess the degradation of silicate-based coatings in combustion environments. Journal of the European Ceramic Society. 2015. 35:4259–4267.

4. Webster RI, Opila EJ. Mixed phase ytterbium silicate environmental-barrier coating materials for improved calcium–magnesium–alumino-silicate resistance. Journal of Materials Research. 2020. 35(17):2358-2372. https://doi.org/10.1557/jmr.2020.151

5. Ridley M, Opila EJ. Microstructural Evolution of Yb2Si2O7 in High Temperature High Velocity Water Vapor. Journal of the European Ceramic Society. 2020. https://doi.org/10.1016/j.jeurceramsoc.2020.05.071

6. Praxair Surface Technologies. Ytterbium monosilicate powder (lot # 03-P5888SG). Ytterbium disilicate powder (lot # 03-P7282BM).

7. Dos Santos e Lucato, SL, Sudre, OH, Marshall, DB. A method for assessing reactions of water vapor with materials in high-speed, high-temperature flow. Journal of American Ceramic Society. 2011. (94): s186-s195.

8. Golden RA, Opila EJ. A method for assessing the volatility of oxides in high-temperature high-velocity water vapor. Journal of European Ceramic Society. 2016;36(5):1135–1147. https://doi.org/10.1016/j.jeurceramsoc.2015.11.016

9. Golden, Rob. Matrix Development for Water Vapor Resistant SiC-Based Ceramic Matrix Composites. Ph.D. Dissertation. University of Virginia. Department of Materials Science and Engineering. https://doi.org/10.18130/V3B34Z

10. Parker CG, Opila EJ. Stability of the Y2O3-SiO2 system in high-temperature, high-velocity water vapor. J Am Ceram Soc. 2019. https://doi.org/10.1111/jace.16915